Structure and Infrastructure Engineering
Vol. 7, Nos. 1–2, January–February 2011, 109–119

Seismic performance of concrete structures exposed to corrosion: case studies of low-rise precast buildings

Fabio Biondini[a], Alessandro Palermo[b]* and Giandomenico Toniolo[a]

[a]*Department of Structural Engineering, Politecnico di Milano, Piazza L. da Vinci, 32 – 20133 Milan, Italy;* [b]*Department of Civil and Natural Resources Engineering, University of Canterbury, Christchurch, 8140, New Zealand*

(*Received 12 May 2009; final version received 16 December 2009; published online 6 April 2010*)

The structural members of precast one-storey or low-rise multi-storey concrete frames for industrial or commercial buildings are often directly exposed to the environment without any protection. The aim of this paper is to investigate the seismic performance of this type of structure considering the material degradation induced by the diffusive attack of aggressive agents, like sulphate and chloride, that may lead to deterioration of concrete and corrosion of reinforcement. The time-variant structural performance of the critical cross-sections of the columns, where plastic hinges are expected to occur during a seismic event, is investigated in terms of bending moment versus curvature relationships. Push-over and push-pull cyclic analyses are then carried out over the structural lifetime to assess the global structural performance in terms of base shear forces and displacement ductility. In this way, even though the lifetime evolution of the dynamic behaviour under ground motion is not captured, it can be shown how the hierarchy of member strengths, and hence the energy-dissipating failure mode claimed for a capacity design of the structure, can be affected by the time-evolution of damage. The proposed procedure is applied to investigate the lifetime seismic performance of one-storey and three-storey frame structures. The results show a significant reduction of both base shear strength and displacement ductility over the structural lifetime and highlight the importance of a lifetime approach to seismic assessment and design of concrete structures.

Keywords: concrete structures; precast buildings; seismic response; aggressive agents; structural damage; lifetime performance

Introduction

Precast concrete structures are quite widespread in Italy and other seismic countries in southern Europe, both for commercial and industrial buildings. These structures are generally limited to two or three storeys and, particularly for industrial use, most of them consist of one-storey hinged frames. The structural members are generally prefabricated, and dry connections with mechanical devices between such members are adopted. Beam-to-column connections are usually hinged and designed to transfer shear only. The dissipative zones are located at the base of the columns, where plastic hinges are expected to develop when a strong earthquake occurs. For these systems, a capacity design based on a collapse mechanism involving the maximum number of storeys is required to optimise the seismic performance (Biondini *et al.* 2010). In several seismic regions outside Europe, including United States, South America, New Zealand, and Japan, precast concrete multi-storey buildings are used also for residential purposes. These systems are usually realised with cast-in-place moment resisting beam-to-column connections to emulate the structural behaviour of typical reinforced concrete monolithic frames (fib 2003), for which the optimal failure mechanism can be selected based on a classical capacity design with strong columns and weak beams (Pauley and Priestley 1992).

Recent research investigations demonstrated that precast structures, under condition of a proper capacity design of connections, can achieve the same seismic performance of cast-in-place structures in terms of global strength and ductility (Biondini and Toniolo 2009). However, if interior concrete panels or masonry/concrete bricks are used as façade elements, the structural members of the building may be directly exposed to the environment without any protection. In such conditions, the diffusive attack from external aggressive agents, like sulphate and chloride, can take place and lead to deterioration of concrete and corrosion of reinforcement (CEB 1992). Such damage can significantly reduce local strength and ductility and modify, in this way, the failure mechanism and the corresponding seismic performance during the structural lifetime (Biondini and Frangopol 2008). As a consequence, capacity design criteria should be

*Corresponding author. Email: alessandro.palermo@canterbury.ac.nz

ISSN 1573-2479 print/ISSN 1744-8980 online

DOI: 10.1080/15732471003588437
http://www.informaworld.com

properly calibrated to consider the severity of environmental exposure and the required structural lifetime.

In this study, the effects of structural damage on the lifetime seismic performance of precast structures are investigated. The lifetime structural analyses are carried out by using a general method for concrete structures in aggressive environments proposed in Biondini *et al*. (2004, 2006). Based on this method, the time-variant performance of the critical cross-sections of the columns is analysed in terms of bending moment versus curvature relationships. The results are used to formulate a structural model based on lumped plasticity finite beam elements, already validated with reference to experimental full-scale tests on structural prototypes for industrial buildings (Palermo *et al.* 2007).

Push-over and push-pull cyclic analyses are therefore carried out over the structural lifetime to assess the global structural performance in terms of base shear forces and displacement ductility. This approach does not allow to capture the dynamic structural behaviour under ground motion. Nevertheless, the results obtained by this type of non-linear static analyses may have important implications for seismic design of structures for which a prescribed distribution of seismic forces can reliably be assumed, as is the case with regular frame buildings. In fact, for relatively flexible systems with high vibration periods, such as those considered in this study, the displacement ductility represents the reducing behaviour factor to be applied to the design static forces corresponding to the peak acceleration of the structure subjected to the ground motion (Paulay and Priestley 1992). Moreover, the results of time-variant non-linear static analyses can show how the hierarchy of member strengths, and hence the energy-dissipating failure mode claimed for a capacity design of the structure, can be affected by the time-evolution of damage.

The proposed procedure is applied to investigate the lifetime seismic performance of one-storey and three-storey precast frame structures. The results show a significant reduction of both base shear strength and displacement ductility over the structural lifetime, with redistribution of the internal forces and alteration of the failure mechanism. It is worth noting that these results need to be validated in quantitative terms by means of a proper calibration of the deterioration model with experimental data, and are limited to the case of regular low-rise frame structures for which the lifetime evolution of the dynamic behaviour under ground motion is not studied. However, in spite of these restrictive conditions, the investigated case studies highlight the importance of a lifetime approach to seismic assessment and design of concrete structures for which the severity of environmental exposure and the required service lifetime are properly taken into account.

Lifetime structural performance of concrete cross-sections

Case study

The lifetime bending performance of a concrete square cross-section with side $b = 70$ cm and reinforced with eight steel bars with diameter $\varnothing = 22$ mm, as shown in Figure 1(a), is investigated.

For concrete, the stress-strain diagram is described by the Saenz's law in compression and by an elastic perfectly plastic model in tension, with (CEN-EN 1992-1-1 2004): compression strength $f_c = 35$ MPa; tension strength $f_{ct} = 0.25 f_c^{2/3}$; initial modulus $E_{c0} = 9500 f_c^{1/3}$; peak strain in compression $\varepsilon_{c0} = 0.20\%$; unconfined strain limit in compression $\varepsilon_{cu} = 0.35\%$; strain limit in tension $\varepsilon_{ctu} = 2f_{ct}/E_{c0}$. The effects of confinement are taken into account by assuming the confined strain limit in compression ε_{cu}^* as a function of the stirrup mechanical ratio ω_w as follows (CEB 1985):

$$\varepsilon_{cu}^* \cong \varepsilon_{cu} + 0.05\omega_w \tag{1}$$

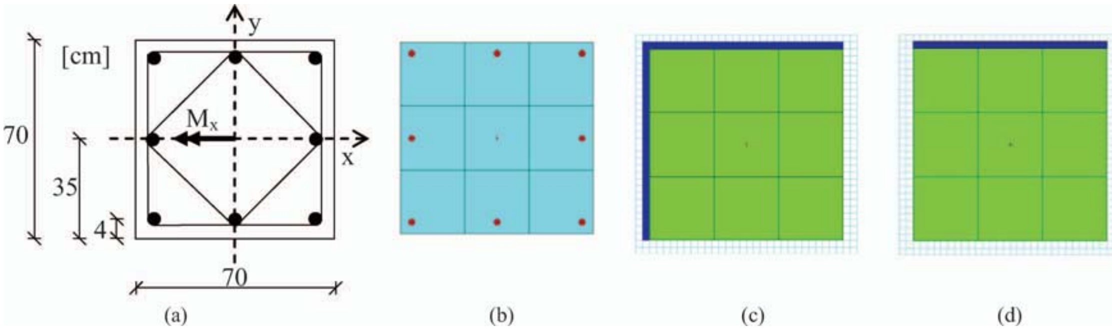

Figure 1. Concrete cross-section. (a) Geometry and reinforcement layout. (b) Structural model. Grid of the cellular automaton and location of the aggressive agent for the cross-section exposed along (c) two sides, and (d) one side.

where ω_w is computed for stirrups Ø8/75 mm. By assuming a low axial force, the effect of confinement on concrete strength is not considered. For steel, the stress-strain diagram is described by an elastic perfectly plastic model in both tension and compression, with: yielding strength $f_{sy} = 430$ MPa; elastic modulus $E_s =$ 206 GPa; strain limit $\varepsilon_{su} = 6.00\%$.

The time-variant structural analysis is carried out based on the model shown in Figure 1(b), where the concrete cross-section is subdivided in quadrilateral isoparametric sub-domains and a numerical integration is performed in each domain by using a 5 × 5 Gauss-Lobatto integration scheme.

Simulation of the diffusion process

The diffusion process is described by the Fick's law (Glicksman 2000):

$$D\nabla^2 C = \frac{\partial C}{\partial t} \tag{2}$$

where D is the diffusivity coefficient, $C = C(\mathbf{x}, t)$ is the concentration of the aggressive agent at point $\mathbf{x} = (x,y)$ and time t, $\nabla C = \mathbf{grad}\ C(\mathbf{x}, t)$, and $\nabla^2 = \nabla \cdot \nabla$. Based on the approach originally proposed in Biondini *et al.* (2004), this process is reproduced numerically by using a special class of evolutionary algorithms called cellular automata (Wolfram 1994). In its basic form, a cellular automaton consists of a regular uniform grid of cells with a discrete variable in each cell which can take on a finite number of states. During time, cellular automata evolve in discrete time steps according to a set of local evolutionary rules. For the diffusion problem in two-dimensions the following evolutionary rule can be adopted (Biondini *et al.*, 2004):

$$C_{ij}^{k+1} = \phi_0 C_{ij}^k + \frac{1-\phi_0}{4}\left(C_{i,j-1}^k + C_{i,j+1}^k + C_{i-1,j}^k + C_{i+1,j}^k\right) \tag{3}$$

where the discrete variable $C_{ij}^k = C(\mathbf{x}_{ij}, t_k)$ represents the concentration in the cell (i, j) at point $\mathbf{x}_{ij} = (x_i, y_j)$ and time t_k, and $\phi_0 \in [0; 1]$ is a suitable evolutionary coefficient. To regulate the process according to a given diffusivity D, the grid dimension $\Delta x = \Delta y$ and the time step Δt of the cellular automaton must satisfy the following relationship:

$$D = \frac{1-\phi_0}{4}\frac{\Delta x^2}{\Delta t} \tag{4}$$

The deterministic value $\phi_0 = 1/2$ usually leads to a good accuracy of the automaton, but the stochastic effects in the local random variability of material diffusivity D induced by cracking can also be taken into account by assuming ϕ_0 as random variable (Biondini *et al.* 2004).

With reference to a diffusivity coefficient $D = 10^{-11}$ m^2/sec, a cellular automaton defined by a grid dimension $\Delta x = 25$ mm and a time step $\Delta t = 0.25$ years is adopted for the cross-section shown in Figure 1(a). The cross-section is assumed to be exposed along two adjacent sides, as shown in Figure 1(c), or only one side, as shown in Figure 1(d), with prescribed concentration C_0 of the aggressive agent. Based on this modelling, the concentration $C = C(\mathbf{x}, t)$ is obtained. Figure 2 shows the maps of concentration $C(\mathbf{x},t)/C_0$ for the two investigated damage scenarios.

Damage modelling and lifetime performance

Structural damage induced by diffusion can be modelled by introducing a degradation law of the effective resistant areas for concrete matrix and steel bars (Biondini *et al.* 2004). This degradation is effectively described by means of a dimensionless damage index $\delta = (\mathbf{x},\ t)$ which provide a direct measure of damage within the range [0; 1]. The damage rates of the materials depend on the mass concentration $C = C(\mathbf{x}, t)$ of the aggressive agent (Bertolini *et al.* 2004). Based on available data for corrosion rate under sulphate and chloride attacks (Pastore and Pedeferri 1994), a linear approximation of the dependency between damage rate and mass concentration is assumed:

$$\frac{\partial \delta(\mathbf{x}, t)}{\partial t} = rC(\mathbf{x}, t) \tag{5}$$

where r is a damage coefficient. In this study, the values $r = 0.04/C_0$ and $r = 0.02/C_0$ are adopted for concrete and steel, respectively. Such values are chosen so to reproduce, for the prescribed concentration C_0, a deterioration process with severe damage of materials, as may occur for carbonated or heavily chloride-contaminated concrete and high relative humidity (Bertolini *et al.* 2004).

Figures 3(a) and 3(b) show the time evolution of the structural performance during the first 50 years of lifetime, with time step of 10 years, in terms of bending moment M_x versus curvature χ_x diagrams under an axial force $N = 500$ kN for the cross-section exposed along two sides (Figure 3(a)) or one side (Figure 3(b)). Since the cross-section exposure to the aggressive agent is not symmetric with respect to the x-axis, the bending moment-curvature diagrams show a different behaviour over the lifetime for $M_x > 0$ and $M_x < 0$. In particular, a higher reduction of the strength capacity

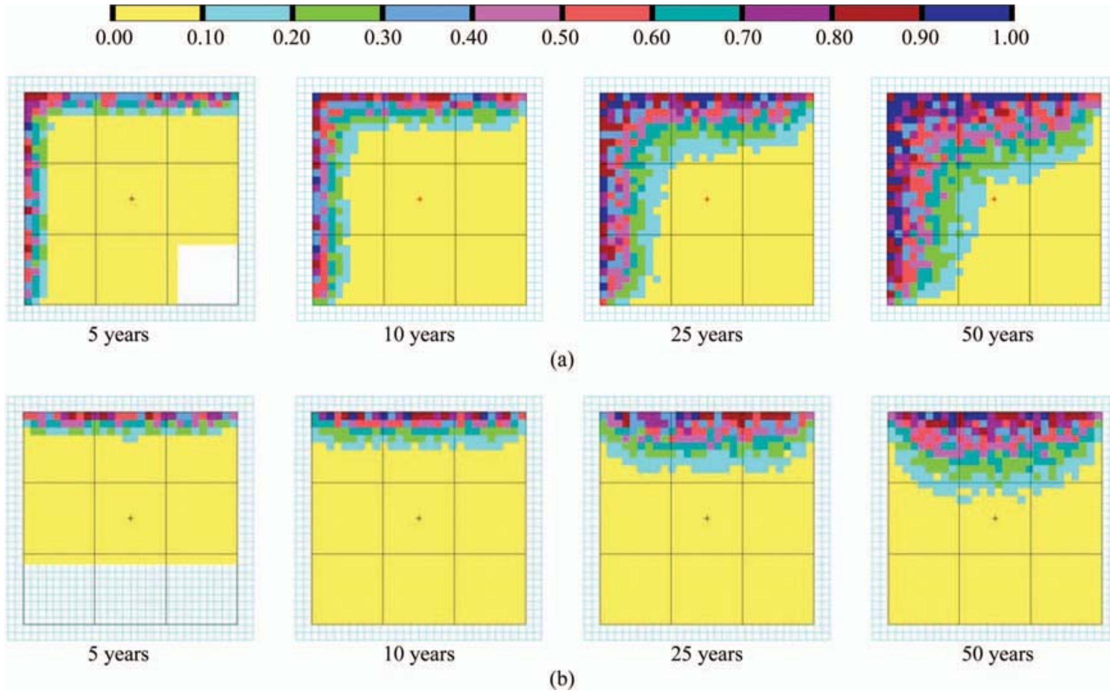

Figure 2. Maps of concentration $C(\mathbf{x}, t)/C_0$ of the aggressive agent after 5, 10, 25, and 50 years from the initial time of diffusion penetration for the cross-section exposed along (a) two sides, and (b) one side.

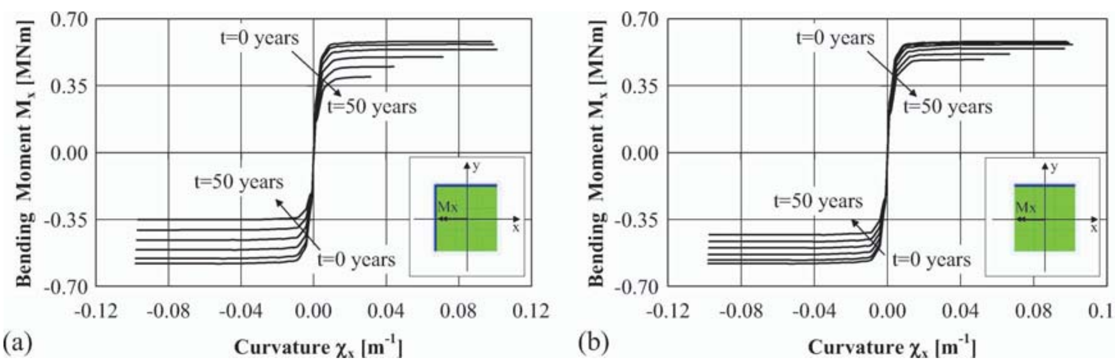

Figure 3. Time evolution with step 10 years of the bending moment M_x versus curvature χ_x with axial force $N = 500$ kN for the cross-section exposed along (a) two sides, and (b) one side.

is achieved for $M_x < 0$, since the bars in tension are located in the most exposed part of the cross-section. For the ultimate curvature at collapse an opposite trend is observed. In fact, for $M_x > 0$ the ultimate curvature is drastically reduced over the lifetime since failure is governed by the concrete crashing of the compressive zone in the most exposed part. These aspects are highlighted in Figures 4 and 5 which show the time-evolution of the maximum resistant bending moment M_R (Figure 4) and curvature ductility μ_χ (Figure 5) given by the ratio of curvatures at ultimate and yielding, respectively, for three values of the axial force $N = 250$, 500, and 750 kN.

Lifetime seismic performance of precast concrete frames

Based on the time-variant analysis on the column cross-sections in correspondence of the critical zones, where formation of plastic hinges can occur, the lifetime seismic performance is herein investigated at the structural level for two case studies: a one-storey

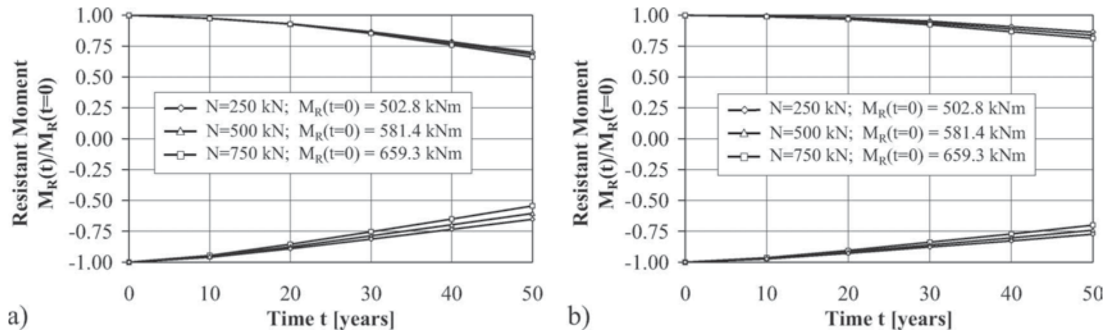

Figure 4. Time evolution of the resistant bending moment M_R with axial force $N = 250$ kN, $N = 500$ kN, and $N = 750$ kN, for the cross-section exposed along (a) two sides, and (b) one side.

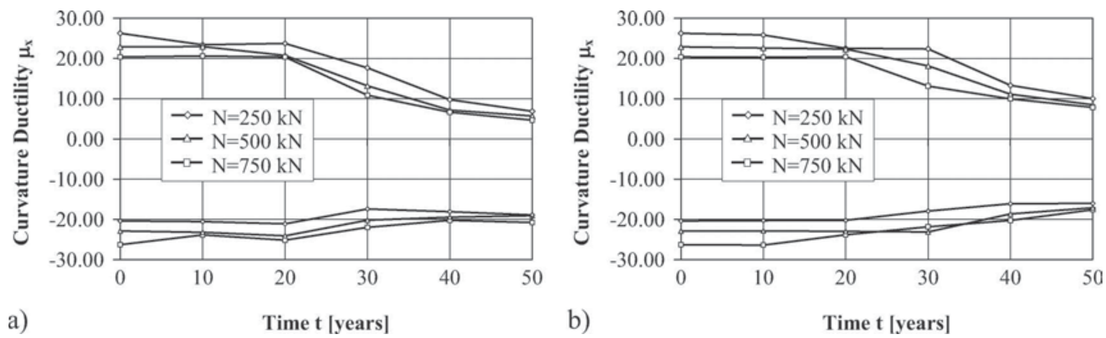

Figure 5. Time evolution of the curvature ductility μ_χ with axial force $N = 250$ kN, $N = 500$ kN, and $N = 750$ kN, for the cross-section exposed along (a) two sides, and (b) one side.

precast concrete frame, typical of European prefabrication for industrial buildings (fib 2008), and a three-storey precast concrete frame, with emulative cast-in-place beam-to-column joints (fib 2003).

Structural modelling

Numerical non-linear analyses are carried out based on the lumped plasticity modelling implemented in the numerical code Ruaumoko 3D (Carr 2006). The cyclic behaviour of the plastic hinge, i.e. rotational inelastic springs, is defined by the relationship between moment and rotation achieved by means of integration of the bending moment-curvature hysteresis rule. The integration is developed by assuming a parabolic distribution of the curvature along a fixed length region of the plastic hinge L_p evaluated as proposed in Paulay and Priestley (1992). The parabola is defined by the curvature values at the two extremities of the plastic hinge length and by a zero value of the first derivative at the extremity with a lower value of curvature.

Before implementation, the bending moment-curvature relationships need to be linearised, as shown in Figure 6. The main parameters, as the initial stiffness, the cracking and the yielding moments M_{crack} and M_{yield}, respectively, the yielding and ultimate curvatures χ_{yield} and χ_{ult}, respectively, are calibrated from the diagrams shown in Figure 3. The cyclic behaviour of the plastic hinges is defined based on the Fukada hysteresis rule (Fukada 1969) by assuming a time-invariant factor $\beta = 0.2$ for stiffness upon load reversal, as typical for beams and columns with low axial loading.

Case study 1: 3D one-storey frame

The lifetime seismic performance of the 3D one-storey frame for industrial building shown in Figure 7 is investigated. The structure has in-plan dimensions 35.0 m × 28.7 m and consists of five planar frames located in the Y direction. Each frame is composed of two columns, with height $h = 11.0$ m and the cross-section shown in Figure 1(a), connected by an I-beam with variable longitudinal profile. The planar frames are connected in the X direction by ribbed roof elements with span $l = 7.0$ m. The structural model is shown in Figure 8. Axial forces $N_1 = 500$ kN and $N_2 = 750$ kN, due to both dead and live loads, are

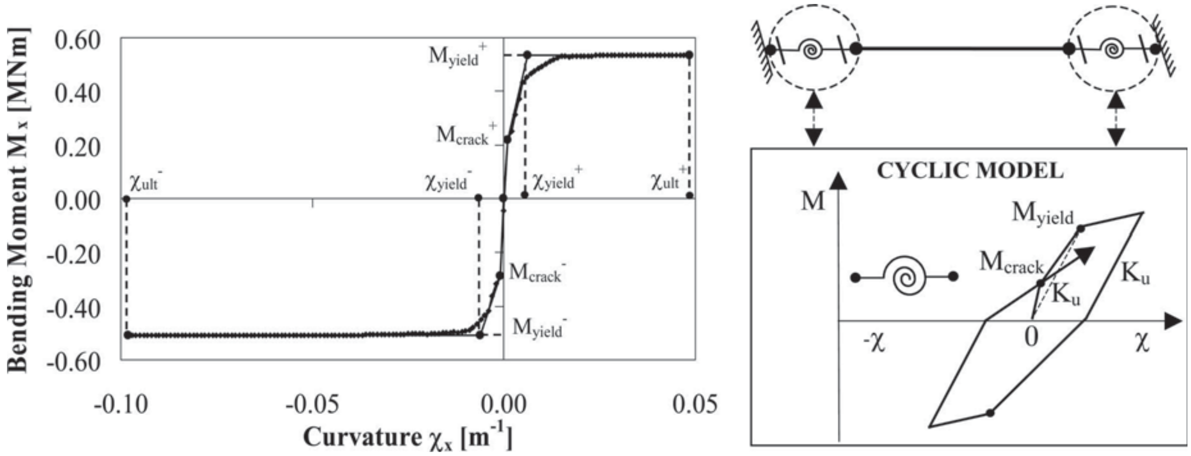

Figure 6. Stepwise linearisation of the bending moment–curvature $M_x - \chi_x$ diagrams.

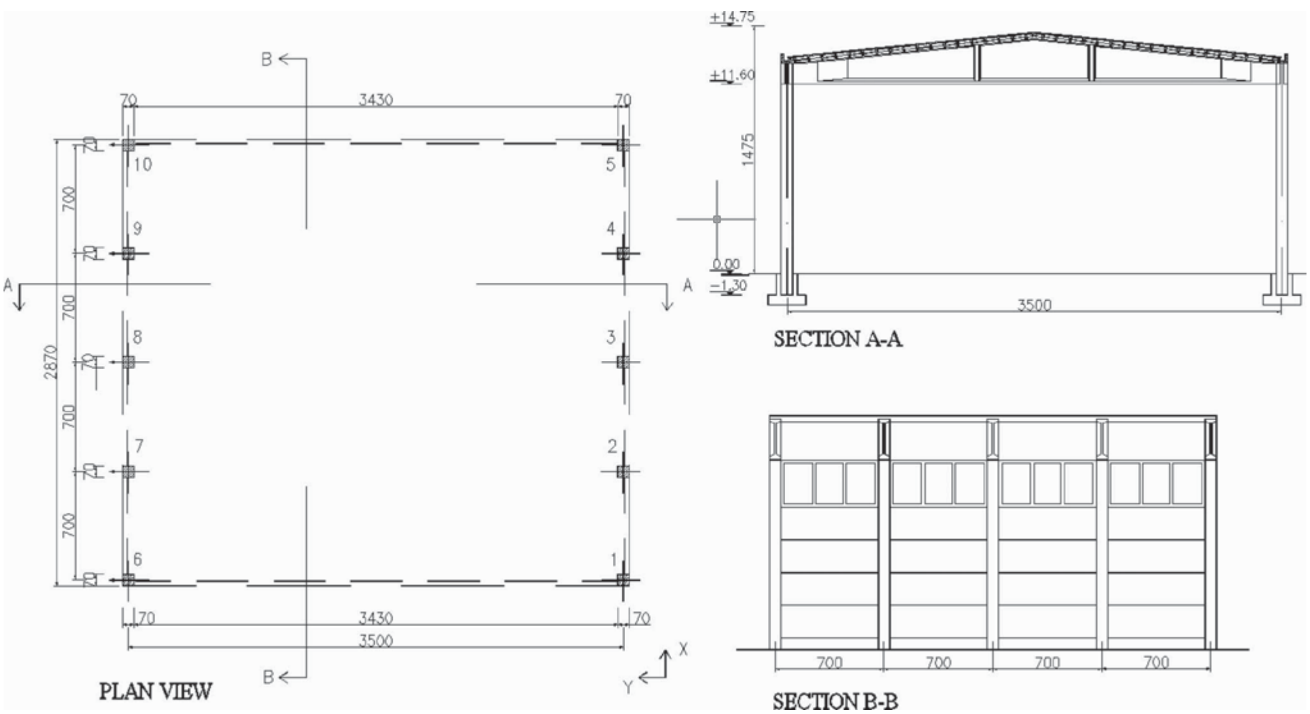

Figure 7. Plan view and transversal sections of the precast one-storey frame structure [m].

applied to the columns of the external and internal planar frames, respectively. Beam-column connections and roof-beam connections are hinged. Due the similar structural scheme in both X and Y directions, only the seismic performance in the Y direction is investigated. It is assumed that the lifetime material degradation affects the columns only, since they are the structural elements directly exposed to the environment. As shown in Figure 9, the columns are exposed along two sides for the external frames (Figures 1(c) and 2(a)), and along one side for the internal frames (Figures 1(d) and 2(b)).

The structure is modelled with elastic beam-type elements and with lumped inelastic rotational springs to simulate the cyclic behaviour of the plastic hinges, as shown in Figure 8. In more detail, for the columns, where a formation of plastic hinges is expected to occur near the foundations, a linear elastic element (cracked second moment of areas, $I_x = I_y = 0.4$, $I_g = 0.4b^4/12$) with an inelastic rotational spring at its base

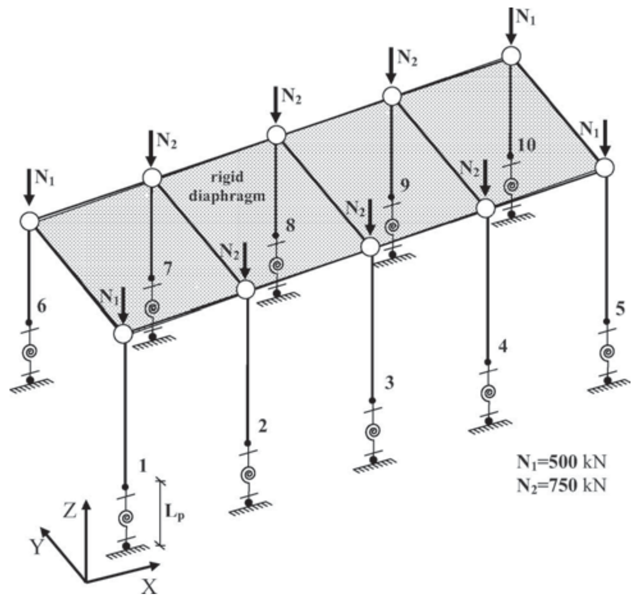

Figure 8. Lumped plasticity model of the one-storey frame.

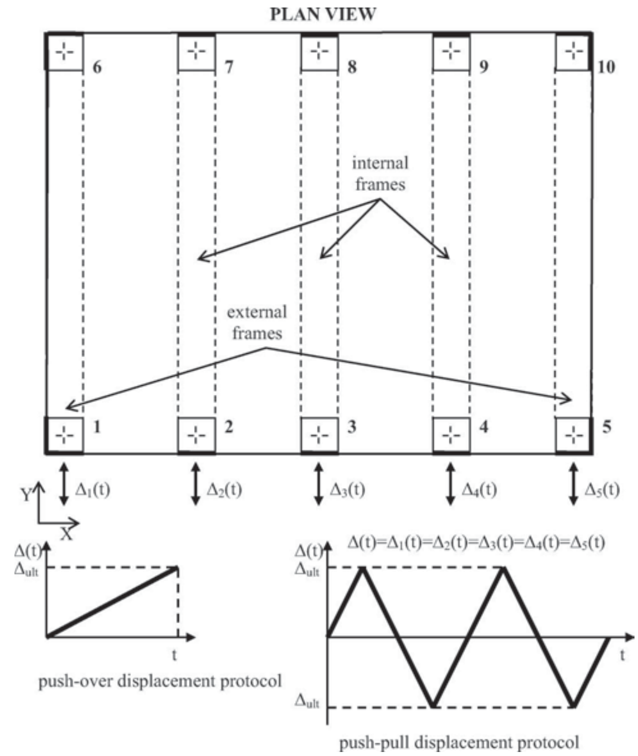

Figure 9. Plan view of the one-storey frame and displacement loading protocol for the push-pull cyclic analysis.

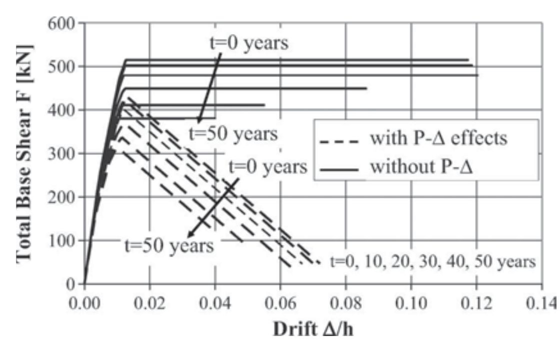

Figure 10. Time evolution of the total base shear force F versus column drift Δ over column height h.

is adopted. The beams are modelled with linear-elastic beam-type elements (uncracked second moment of areas $I_x = I_y = I_g$). A rigid diaphragm constraint is assumed between the planar frames due to the high axial stiffness of the roof elements. Push-over non-linear static analyses, as well as push-pull cyclic analyses based on the loading displacement protocol shown in Figure 9, are carried out by taking the second order geometrical effects (P-Δ effects) into account.

Figure 10 shows the results of the lifetime push-over analysis in terms of total base shear versus drift, or top column displacement over column height ratio, with and without P-Δ effects. A significant performance reduction over time is obtained. In particular, Figure 11 shows that material degradation leads to a significant strength reduction (Figure 11(a)), as well as to a shear force redistribution among frames (Figure 11(b)). In fact, due to the higher axial load ($N_2 = 750$ kN for internal columns, $N_1 = 500$ kN for external columns), the P-Δ effects are more important for the internal frames and, up to 40 years of lifetime, the collapse of the structure is governed by the instability failure of columns 7, 8, and 9. This leads to an increment of the percentage of shear force in the external frames. On the contrary, since the external columns are more exposed to the environmental conditions, after 40 years of lifetime and up to 50 years the collapse of the structure is characterised by a material failure of columns 6 and 10 and, consequently, a higher percentage of shear force is provided by the internal frames.

It is worth noting that the collapse of the structure is governed by columns 6 to 10, and not columns 1 to 5, because of the direction of loading assumed for push-over analysis. In fact, since the moment-curvature behaviour is not symmetrical (see Figure 3), a higher reduction of ultimate curvature, hence curvature ductility, occurs for bending behaviour of columns 6 to 10 with $M_x > 0$.

Moreover, Figure 12 shows that material degradation leads also to a significant reduction over time of both the ultimate drift (Figure 12(a)) and displacement ductility (Figure 12(b)), with the most important effects during the first 20 to 30 years of lifetime. As already pointed out, such results can have important

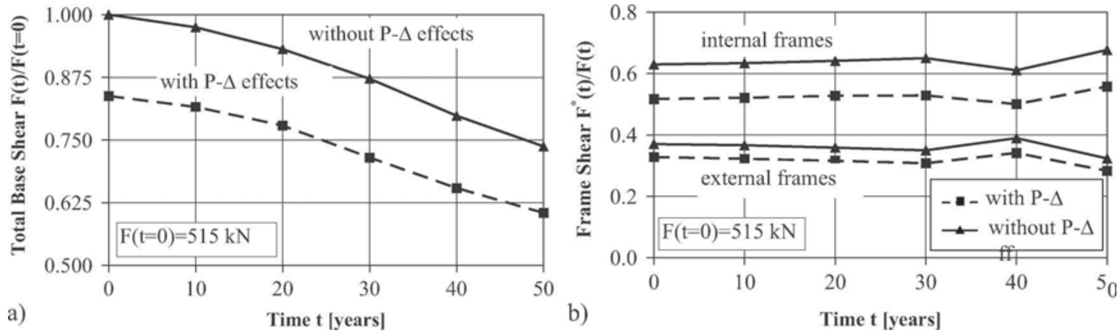

Figure 11. Time evolution of dimensionless base shear forces. (a) Maximum total shear force $F(t)$. (b) Maximum frame shear forces $F^*(t)$.

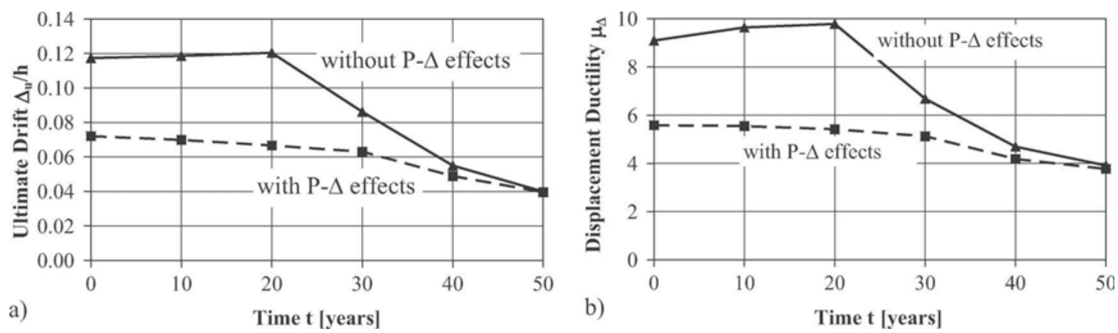

Figure 12. Time evolution of (a) ultimate drift Δ_u and (b) displacement ductility μ_Δ.

implications in seismic design procedures based on linear static analysis since for relatively flexible systems with high vibration periods, as those considered in this study, the displacement ductility represents the reducing behaviour factor to be applied to the static forces corresponding to the peak acceleration of the structure subjected to the ground motion.

The results of the push-pull cyclic analysis are finally shown in Figure 13 in terms of base shear versus drift for the two lifetime steps 0 and 50 years. A remarkable reduction of the energy dissipation capacity after 50 years of lifetime is obtained, as emphasised by the shaded areas shown in Figures 13(a) and 13(b), which correspond to values of equivalent viscous damping $\xi_{equiv} = 30.8\%$ and $\xi_{equiv} = 27.6\%$, respectively.

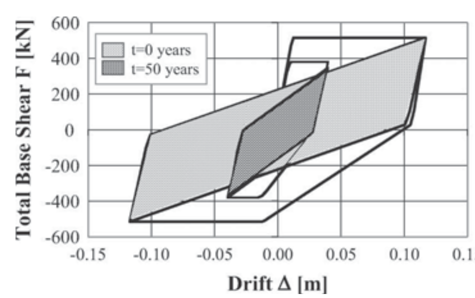

Figure 13. Total base shear F versus column drift Δ for the push-pull cyclic test for $t = 0$ and $t = 50$ years.

Case study 2: 2D three-storey frame

The 2D three-storey precast concrete frame shown in Figure 14 is considered. The columns have inter-storey height $h = 4.0$ m and the cross-section shown in Figure 1(a). The beams have a span of $l = 8.0$ m and rectangular section 0.5 × 0.8 m. An axial load N_1 250 kN, due to both dead and live loads, is applied to the columns at each storey level. Cast-in-place moment resisting beam-to-column connections are adopted to emulate the structural behaviour of monolithic frames. The connections are designed according to capacity design criteria, i.e. strong column – weak beam, by assuming for beams a suitable over-strength ratio γ_c in terms of design resistant bending moments M_{rd}:

$$\gamma_c = \frac{\left|M_{rd}^{columns}\right|}{\left|M_{rd}^{beams}\right|} \tag{6}$$

Two cases are investigated by assuming $\gamma_c = 1.1$ and $\gamma_c = 1.3$, as suggested by European seismic codes

(CEN-EN 1998-1 2004) for structures with low ductility class and high ductility class, respectively. Based on the resistant bending moments of the undamaged cross-sections of the columns, as indicated in Figure 4, the resistant bending moments of the beams listed in Table 1 are chosen for the two cases studied.

Lifetime material degradation is assumed to affect the columns only, with the aggressive agent acting on the external edge of the column cross-sections (Figures 1(d) and 2(b)). The corresponding time evolution of the over-strength factor γ_c associated to each storey is shown in Figure 15. It is noted that the higher is the axial load in the column cross sections, the greater is the reduction of the over-strength factor γ_c. In particular, a change of collapse mechanism may occur for $\gamma_c < 1$, since the capacity design criterion of strong column–weak beam no longer holds. To investigate this aspect a push-over non-linear analysis is carried out.

Table 1. Resistant bending moments of the beams for the frame shown in Figure 14.

	M_{b1} [kNm]	M_{b2} [kNm]	M_{b3} [kNm]
Low ductility	1127.9	985.6	457.1
High ductility	954.4	834.0	386.8

To this aim, as shown in Figure 14, the frame is modelled with elastic beam-type elements and with lumped inelastic rotational springs to simulate the non-linear behaviour due to the formation of plastic hinges. For columns and beams, a linear elastic element (cracked second moment of areas, $I_x = I_y = 0.4I_g$) with inelastic rotational springs at the ends where formation of plastic hinges is expected, are adopted. The second order geometrical effects (P-Δ effects), which are less relevant compared to the previous case study, are neglected. Based on this modelling, a push-over analysis with a linear distribution of applied forces, as shown in Figure 14, is carried out by monotonically increasing the intensity of the horizontal forces up to failure.

The results are shown in Figure 16 in terms of total base shear versus top displacement for the low ductility frame. A significant reduction of the total base shear strength, even thought gradual, is observed over the structural lifetime. Moreover, an abrupt reduction of the ultimate displacement and hence of the

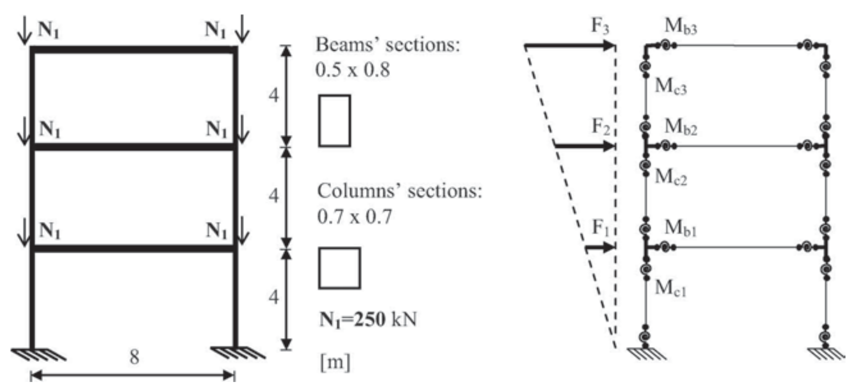

Figure 14. Geometrical data and modelling of the three-storey concrete frame structure.

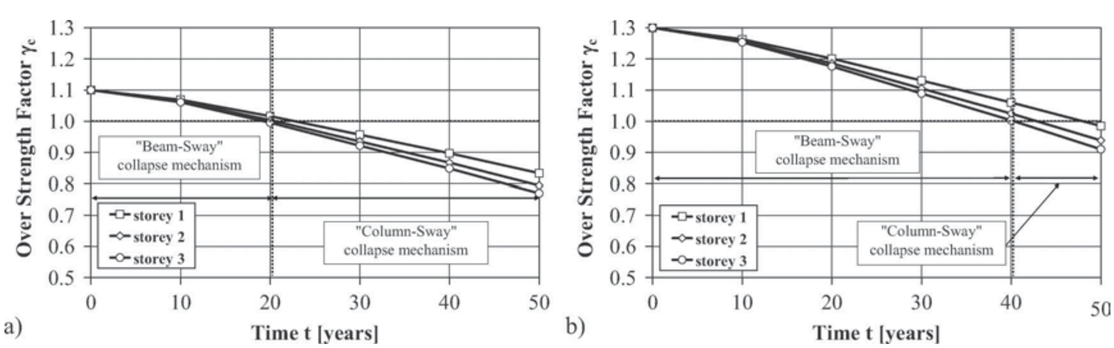

Figure 15. Time evolution of the over-strength factor γ_c: (a) low ductility; (b) high ductility.

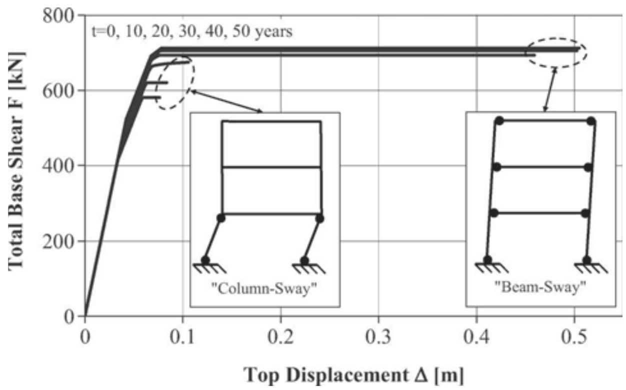

Figure 16. Total base shear F versus top displacement Δ for the low ductility frame.

displacement ductility is obtained after about 20 to 30 years. In fact, as expected, due to the reduction of bending moment capacity of the columns, a change of collapse mechanism occurs moving from a typical 'beam sway' to a 'column sway' mechanism. As a consequence, since the overall dissipation capacity is totally lumped at the bottom of the columns, with all beams in the elastic range, a brittle failure occurs with displacement ductility around 1.5. Similar results are obtained for the high ductility frame, even if with a change of collapse mechanism delayed over time. These results demonstrate the importance of taking the severity of environmental exposure and the required service lifetime into account in seismic design of structures.

Conclusions

The lifetime seismic performance of concrete structures under diffusive attack of aggressive agents has been investigated. Non-linear static analyses have been carried out up to collapse over the structural lifetime to evaluate the effects of damage on the time evolution of both ductility resources and hierarchy of member strengths. The results obtained for one-storey and three-storey precast frame structures showed a significant reduction of both shear strength and displacement ductility over the structural lifetime, with redistribution of the internal forces and alteration of the energy-dissipating failure mode claimed for a capacity design of the structure. These results need to be validated in quantitative terms by means of a proper calibration of the deterioration model with experimental data. Moreover, they are limited to the case of regular low-rise frame structures for which the lifetime evolution of the dynamic behaviour under ground motion is not studied, and the effects of reoccurrence of seismic events are not considered. Nevertheless, they effectively highlight the important role of a lifetime approach for both seismic assessment of existing structures and seismic design of new structures. In particular, a revision of the seismic design criteria is recommended for frame systems in terms of both force reducing factors (behaviour factors) at global level, and over-strength factors at local level, since these parameters are expected to vary over time depending on the environmental exposure of the structure. In this perspective, further investigations are needed to properly identify among ordinary precast structures, including multi-storey buildings, the structural typologies more vulnerable to lifetime material degradation effects. To this aim, non-linear time history dynamic analyses under ground excitation are also recommended. Finally, for a rational calibration of the seismic design criteria, a probabilistic framework has to be provided.

Acknowledgements

This study has been supported by Research funds PRIN2005 (prot. 2005082490) from the Italian Ministry of University and Research, and by the National Research Project RELUIS funded by the Department of Civil Protection.

References

Bertolini, L., Elsener, B., Pedeferri, P., and Polder, R., 2004. *Corrosion of steel in concrete*. Weinheim, Germany: Wiley-VCH.

Biondini, F., Bontempi, F., Frangopol, D.M., and Malerba, P.G., 2004. Cellular automata approach to durability analysis of concrete structures in aggressive environments. *Journal of Structural Engineering, ASCE*, 130 (11), 1724–1737.

Biondini, F., Bontempi, F., Frangopol, D.M., and Malerba, P.G., 2006. Probabilistic service life assessment and maintenance planning of concrete structures. *Journal of Structural Engineering, ASCE*, 132 (5), 810–825.

Biondini, F. and Frangopol, D.M., 2008. Probabilistic limit analysis and lifetime prediction of concrete structures. *Structure and Infrastructure Engineering*, 4 (5), 399–412.

Biondini, F. and Toniolo, G., 2009. Probabilistic calibration and experimental verification of the seismic design criteria for concrete frames. *Journal of Earthquake Engineering*, 13, 426–462.

Biondini, F., Toniolo, G., and Tsionis, G., 2010. Capacity design and seismic performance of multi-storey precast structures. *European Journal of Environmental and Civil Engineering*, 14(1), 11–28.

Carr, A.J., 2006. RUAUMOKO program for inelastic dynamic analysis. Department of Civil Engineering, University of Canterbury, Christchurch, New Zealand.

CEB, 1985. *Model code for seismic design of concrete structures*. Bulletin 165.

CEB, 1992. *Durable concrete structures – design guide*. Bulletin 183.

CEN-EN 1992-1-1, 2004. *Eurocode 2: Design of concrete structures. Part 1-1: General rules and rules for buildings*. Brussels: European Committee for Standardisation.

CEN-EN 1998-1, 2004. *Eurocode 8: Design of structures for earthquake resistance. Part 1: General rules, seismic actions and rules for buildings*. Brussels: European Committee for Standardisation.

fib, 2003. Seismic design of precast concrete building structures. State-of-art report prepared by Task Group 7.3. Bulletin 27, October 2003.

fib, 2008. Structural connections for precast concrete buildings. Guide to good practice prepared by Task Group 6.2. February 2008.

Fukada, Y., 1969. Study on the restoring force characteristics and design of reinforced concrete buildings (in Japanese). *Proceedings of the Kanto District Symposium*, Tokyo, Japan, Architectural Institute of Japan. No. 40.

Glicksman, M.E., 2000. *Diffusion in solids*. New York, NY, USA: John Wiley & Sons.

Pastore, T. and Pedeferri, P., 1994. La corrosione e la protezione delle opere metalliche esposte all'atmosfera. *L'edilizia*, December, 75–92 (in Italian).

Paulay, T. and Priestley, M.J.N., 1992. *Seismic design of reinforced concrete and masonry buildings*. New York, NY, USA: John Wiley & Sons.

Palermo, A., Carabellese, A., and Toniolo, G., 2007. Numerical validation of pseudo-dynamic and quasi-static cyclic tests on full-scale precast industrial building prototypes. *Proceedings of the 8th Pacific Conference on Earthquake Engineering*, 5–7 December, Singapore, CD-ROM.

Wolfram, S., 1994. *Cellular automata and complexity – collected papers*. New York, NY, USA: Addison-Wesley.